Proc. Natl. Acad. Sci. USA
Vol. 94, pp. 2817–2822, April 1997
Biochemistry

Supercoiling-dependent flexibility of adenosine-tract-containing DNA detected by a topological method

(DNA bending/DNA topology/site-specific recombination/transcription)

HUA TSEN AND STEPHEN D. LEVENE*

Program in Molecular and Cell Biology, The University of Texas at Dallas, Post Office Box 830688, Richardson, TX 75083-0688

Communicated by Donald Crothers, Yale University, New Haven, CT, January 14, 1997 (received for review July 17, 1996)

ABSTRACT **Intrinsically bent DNA sequences have been implicated in the activation of transcription by promoting juxtaposition of DNA sequences near the terminal loop of a superhelical domain. We have developed a novel topological assay for DNA looping based on λ integrative recombination to study the effects of intrinsically bent DNA sequences on the tertiary structure of negatively supercoiled DNA. Remarkably, the localization of adenosine-tract (A-tract) sequences in the terminal loop of a supercoiled plasmid is independent of the extent of intrinsic bending. The results suggest that A-tract-containing sequences have other properties that organize the structure of superhelical domains apart from intrinsic bending and may explain the lack of conservation in the degree of A-tract-dependent bending among DNA sequences located upstream of bacterial promoters.**

DNA supercoiling is the tertiary winding of the DNA helix axis that occurs when the double helix is under- or overwound. The DNA in essentially all cells in all organisms is supercoiled and the mechanical stress of supercoiling is intimately involved in such central aspects of cellular metabolism as DNA replication, transcription, and recombination. The role of supercoiling in these processes is poorly understood, largely because details of the structure and dynamics of superhelical DNA are just beginning to emerge from a considerable number of experimental and theoretical studies (for review, see refs. 1–3). One factor that is probably critical is that the tertiary structure of supercoiled DNA, which dictates the three-dimensional geometry of DNA segments in space, promotes interactions among proteins bound to specific binding sites that are widely separated along the DNA contour (1, 2, 4).

The main motivation for the studies described herein is the observation that transcription in a number of systems can be regulated by the presence of intrinsically bent adenosine-tract (A-tract)-containing regions located upstream from their respective promoters (5–12) (for review, see ref. 5). For the *Escherichia coli lac* system, Gartenberg and Crothers (10) found that functional replacement of bending induced by catabolite activator protein with an A-tract-dependent bend occurs if the DNA template is supercoiled but not if the template is relaxed, thus, suggesting that the effects of bending and supercoiling are synergistic in this system. Supercoiling could facilitate contact between DNA and the face of RNA polymerase opposite the promoter binding site, which may stabilize the transcription-competent open complex.

The role that bent helical regions play in the organization of DNA tertiary structure has received little experimental attention, possibly because of the paucity of techniques available for characterizing the phenomenon in solution. Laundon and Griffith (13) showed by electron microscopy that embedding two copies of an intrinsically bent segment of kinetoplast DNA in a superhelical plasmid resulted in DNA conformations in which the ends of superhelix branches had a high probability of coincidence with the relative locations of the kinetoplast inserts. Diverse theoretical treatments predict that intrinsic curvature and nonuniform bending rigidity are important features that organize DNA tertiary structure by localization in the terminal loops of superhelical domains (14–20).

Site-specific recombination constitutes a model class of processes for experimentally investigating loop-mediated protein–DNA interactions. Intramolecular site-specific recombination normally involves interactions between sites that are separated by hundreds or thousands of base pairs along DNA. In random-collision site-specific recombination systems, such as the integrative (Int) system of bacteriophage λ, the synapsis of recombination sites located along a supercoiled DNA molecule transiently traps a number of substrate supercoils that are converted by recombination into topologically invariant knot or catenane crossings in the products. The number of trapped supercoils is a fluctuating quantity sampled by linear diffusion of the recombination sites along the contour of the superhelix, a motion termed "slithering" (21). The distribution of product topologies is characterized by gel electrophoresis after the DNA is nicked (Fig. 1). Site-specific recombination can thus be used as a reporter of DNA substrate tertiary structure in solution (21, 22) and *in vivo* (23).

MATERIALS AND METHODS

Plasmid DNA. Three recombination substrates, pA_5N_5i, pA_5N_1i, and pRani, were generated by cloning 105-bp synthetic restriction fragments shown in Fig. 1 into the *Sma*I site of p*att*4.5i, a 4.5-kb pGEM-7Zf(+) derivative. The construction of these plasmids will be described in detail elsewhere. Plasmids were isolated by the alkaline lysis method (24) followed by two rounds of CsCl/ethidium bromide density-gradient centrifugation. Plasmid sequences were confirmed by dideoxynucleotide sequencing (24).

Recombination Assays. Recombination reactions contained 0.5 μg of plasmid DNA, 50 ng of Int, and 60 ng of *E. coli* integration host factor (IHF) and were incubated for 30 min in 50 mM Tris·HCl/50 mM NaCl/5 mM spermidine/2 mM Na_2EDTA/bovine serum albumin (200 μg/ml)/0.1 mM dithiothreitol, pH 7.5. Int and IHF proteins were gifts or were purified in this laboratory according to modifications of published methods (25–27). Recombination products were subjected to limited digestion with DNase I in the presence of ethidium bromide (28) prior to analysis by agarose gel elec-

The publication costs of this article were defrayed in part by page charge payment. This article must therefore be hereby marked "*advertisement*" in accordance with 18 U.S.C. §1734 solely to indicate this fact.

0027-8424/97/942817-6$2.00/0
PNAS is available online at **http://www.pnas.org**.

Abbreviations: A-tract, adenosine-tract; Int, λ integrative; IHF, integration host factor.

*To whom reprint requests should be addressed. E-mail address: sdlevene@utdallas.edu.

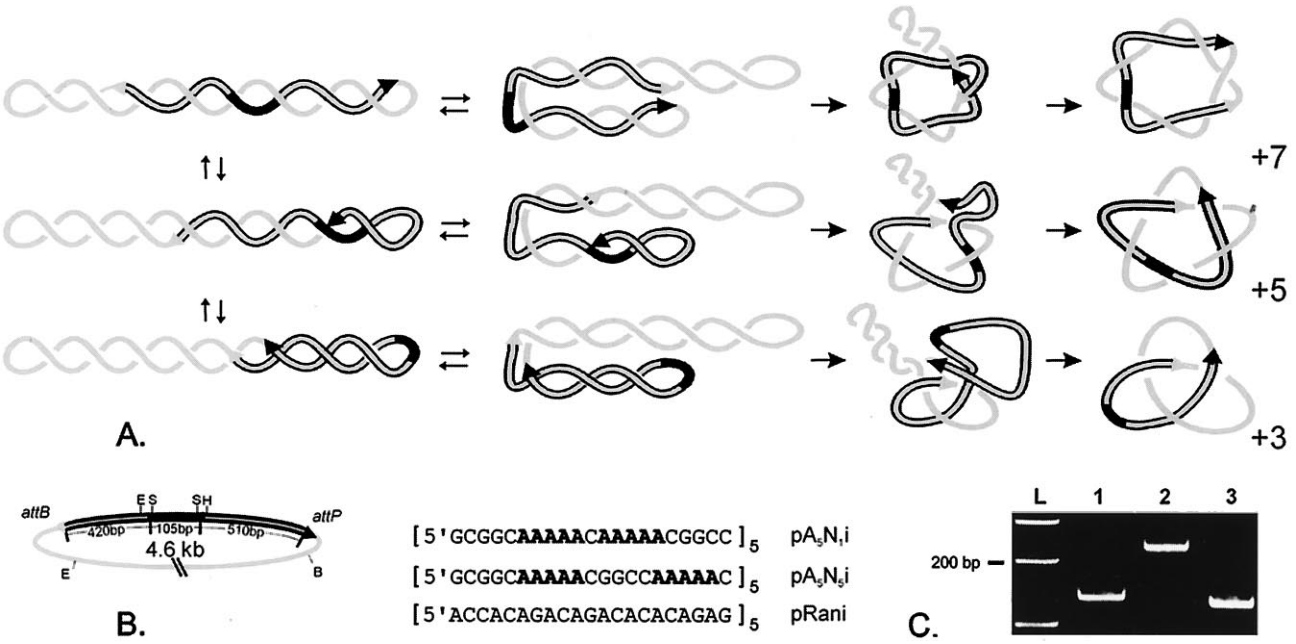

FIG. 1. (*A*) Topology of "random-collision" site-specific recombination. The diagram shows a planar projection of a prototypical supercoiled DNA substrate undergoing intramolecular site-specific recombination. Recombination sites, indicated by arrowheads, divide the DNA contour into two distinct domains, shown as shaded and outlined regions. Relative motion of these sites along the superhelix axis is termed slithering (first column). This motion generates a variable number of interdomainal superhelical turns, which are trapped at site synapsis in the folded conformations (second column). Recombination (third column) and subsequent nicking of the DNA to remove residual supercoiling (fourth column) generates knotted products in which the signed number of irreducible knot crossings (*Kn*, given below and to the right of each knot) is proportional to the number of interdomainal supercoils trapped at synapsis. Additional supercoiling-independent crossings appear in each product as a consequence of the mechanism of recombination. The presence of a bent or flexible insert, indicated by the solid segment, can bias the distribution of knotted products by localizing in the terminal loops of the superhelix, as in the case of the conformation shown at the bottom. With the symmetrical arrangement of recombination sites shown, the most favorable configurations correspond to juxtaposition of the recombination sites across the superhelix axis, which biases the distribution of recombination products in favor of simple topologies. (*B*) Plasmid DNAs used in these studies. Recombination substrates were derived from a plasmid designated p*att*4.5i, which positions the centers of the *att* sites relative to the *Sma*I (S) cloning site as indicated. A-tract-containing plasmids, pA_5N_5i and pA_5N_1i, and control plasmid pRani were constructed by cloning pentameric repeats of the 21-bp double-stranded oligonucleotide sequences shown into the *Sma*I site of p*att*4.5i. The 105-bp insertions are indicated by the solid segment in the plasmid map. (*C*) Electrophoresis in an 8% polyacrylamide gel of 138-bp *Kpn*I–*Hin*dIII fragments containing synthetic inserts. Lanes: L, 100-bp ladder; 1, $[A_5N_1]_5$; 2, $[A_5N_5]_5$; 3, $[Ran]_5$.

trophoresis. Variability in the efficiency of the nicking reaction, which occasionally left traces of undigested DNA, did not systematically affect the experimental results. Electrophoresis was at 2.5 V/cm for 16–20 h in 0.8% agarose gels in TBE buffer (50 mM Tris-borate/1 mM Na_2EDTA, pH 8.5). After ethidium staining, gel images were captured by using an integrating charge-coupled device video camera. Product distributions were quantitated from the digitized images; normalized knot distributions are plotted as histograms. Additional details concerning the quantitation of knot distributions can be found in ref. 27. All plasmids were adjusted to similar superhelix densities by relaxation with wheat-germ topoisomerase I [purified in this laboratory by the procedure of Dynan *et al.* (29)] in the presence of ethidium bromide. Substrate superhelix densities were determined by two-dimensional agarose gel electrophoresis (30, 31).

Assays for DNA Unwinding. Mixtures of topoisomers were prepared from aliquots of native supercoiled plasmid incubated with wheat-germ topoisomerase I in the presence of ethidium bromide. The topoisomer mixtures were pooled, ethidium was removed by extraction with 1-butanol, and the DNA was analyzed by two-dimensional gel electrophoresis. First-dimension electrophoresis in all cases was carried out at 2 V/cm in 0.8% agarose gels electrophoresed in TBE buffer containing 50 mM NaCl for 11 h with buffer recirculation. Second-dimension electrophoresis was carried out in TBE buffer containing an appropriate concentration of chloroquine phosphate.

S1 nuclease sensitivity assays were carried out by the protocol described by Bowater *et al.* (31). DNA (1 μg) suspended in 20 μl of buffer containing 50 mM sodium acetate, 50 mM NaCl, 5 mM spermidine, 1 mM $ZnCl_2$ (pH 4.5) was incubated at a specified temperature for 5 min, removed to ice, and subsequently incubated with 10 units of nuclease S1 for 30 min at 15°C. The extent of S1 cleavage was examined by electrophoresis on a 0.8% agarose/TBE gel.

Mathematical Modeling of Recombination-Product Distributions. Knot distributions were calculated by using a modification of the slithering model for intramolecular site-specific recombination of a supercoiled substrate molecule (21, 22). The attachment sites can be imagined to divide the DNA contour into two domains; slithering models postulate that the number of irreducible topological crossings generated by recombination of a circular substrate is proportional to the number of interdomainal superhelical turns trapped during recombination-site synapsis. The distribution of interdomainal crossings is given by the fraction of all possible superhelical configurations associated with a given (integral) number of interdomainal superhelical turns and is equal to $n_i\xi_i/\Sigma_i\, n_i\xi_i$, where n_i is the number of configurations with i interdomainal crossings and ξ_i is a bias factor equal to unity for an unbiased substrate. The total slithering-independent contribution to the number of product nodes, which is attributable to wrapping of DNA around the recombination proteins and to the mechanism of recombination, was taken to be equal to -2 (21). Calculated distributions were corrected for the use of heterogeneous topoisomer populations.

RESULTS

Recombination-Product Distributions. We examined the distribution of products generated by *in vitro* Int recombination of several plasmid DNAs. All of the constructs contained Int recombination sites (*attB* and *attP*) in inverse orientation, yielding knotted circular products on recombination (Fig. 1). Two plasmids, pA_5N_5i and pA_5N_1i, were constructed by inserting isomeric 105-bp segments bearing 10 A_5-tracts in a defined context relative to the recombination sites. The A-tracts were repeated either in phase or out of phase with the DNA helix screw, respectively. In pA_5N_5i, the inserted DNA segment containing in-phase repeats of the A_5-tract has a sequence-directed bend of approximately 180° (32), whereas the out-of-phase isomer in pA_5N_1i is intrinsically straight. The extent of intrinsic bending is confirmed by the respective polyacrylamide-gel mobilities of the inserted fragments, as shown in Fig. 1*C*. These A-tract-containing substrates were designed to test the idea that intrinsically bent segments tend to localize in the terminal loops of superhelical domains. With the recombination sites located nearly equidistantly from the center of the A-tract insert this tendency would be revealed as a biased product distribution that favors simple knotted products over more complex knots, as shown in Fig. 1*A*. A control plasmid, pRani, was constructed with a 105-bp insert containing the same number of A·T base pairs as the A-tract isomers but arranged such that every adenosine residue was flanked by either guanosines or cytidines, thus avoiding ApA dinucleotides and A-tracts. The recombination-product distribution of the parent plasmid, p*att*4.5i, which was used to construct these substrates, was also examined.

Agarose gel analyses of several Int recombination reactions are shown in Fig. 2. Int reactions were carried out at several temperatures between 16°C and 37°C to investigate potential effects of temperature on the structure of the A-tracts. The extent of A-tract-induced DNA bending has been shown to be a function of temperature in a number of studies (32–35); in the absence of multivalent metal ions, such as Mg^{2+}, bending decreases with increasing temperature and essentially disappears above 40°C.

Fig. 2 shows that the distributions of knotted products obtained with both of the A-tract-containing plasmids are markedly different from those obtained with the control plasmids, pRani and p*att*4.5i. Relative to controls, the distributions of A-tract-containing products are enriched for less complex knotted forms at the expense of more complex knots. This is clearly revealed in the normalized knot distributions plotted in Fig. 2, where it is evident that the proportion of simple knots increases with increasing temperature. No significant dependence of the knot distribution on temperature was observed with either of the control substrates; the slight increase in simple knots obtained with increasing temperature is consistent with the expected increase in B-DNA helical repeat with temperature. Because the biasing of the knot distribution is independent of A-tract phasing and increases with temperature, the simplest explanation for these observations is that negative supercoiling and increased temperature promote a transition to an altered DNA conformation in A-tract-containing regions. This altered conformation possesses a greater degree of isotropic flexibility than flanking plasmid DNA and hence localizes preferentially in the terminal loops of superhelical domains.

Increased A-Tract Flexibility Does Not Involve Strand Separation. It is possible that the unusual properties of A-tracts in these superhelical molecules can be trivially explained in terms of stable supercoiling-induced unwinding of these sequences, which would be expected to dramatically increase the flexibility of the A-tract-containing regions. Previous studies on supercoiling-induced unwinding of A+T-rich sequences in B-form DNA have shown that the presence of

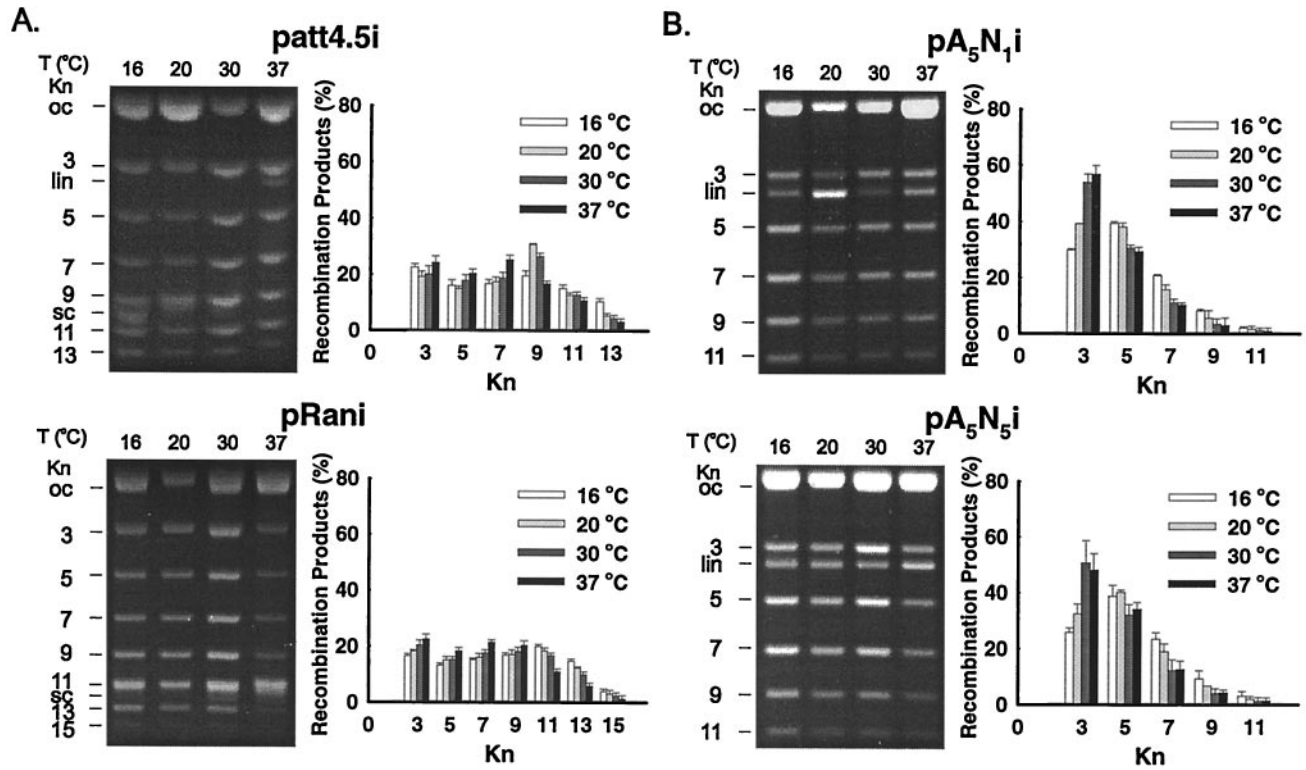

FIG. 2. Recombination-product distributions of four natively supercoiled Int recombination substrates ($\sigma_{avg} = -0.055 \pm 0.005$). (*A*) Control plasmids. (*B*) A-tract-containing plasmids. Each recombination reaction was incubated for 30 min at the indicated temperature and analyzed by agarose gel electrophoresis. The number of irreducible knot crossings, *Kn*, corresponding to each band are shown. Other species are labeled as follows: oc, open-circular (unknotted); lin, linear; sc, supercoiled substrate. Each histogram represents the average of at least three experiments; error bars indicate one standard deviation.

even modest concentrations of monovalent salt (>20 mM NaCl) suppresses stable unwinding of DNA (31). The Int recombination reaction mixtures contain 50 mM NaCl and 5 mM spermidine, thus stable unwinding of the A-tract-containing regions is not expected under these conditions. Moreover, the knot distributions remained unchanged in Int recombination reactions carried out in a buffer that contained 70 mM KCl and 10 mM $MgCl_2$, the latter replacing spermidine as the source of multivalent counterions (data not shown). Nevertheless, we undertook a series of experiments to rule out the possibility of localized strand separation in these plasmids.

Populations of topoisomers of pA_5N_5i and pA_5N_1i were prepared by relaxation of the native plasmids with topoisomerase I in reaction mixtures that contained ethidium bromide at various concentrations. These topoisomer samples were pooled and subjected to two-dimensional agarose gel electrophoresis, as shown in Fig. 3. If a local structural transition (such as strand separation) requires a critical level of supercoiling, then an abrupt change in mobility will be observed at a critical value of the linking difference in the two-dimensional gel pattern (30, 31, 36).

The concentration of chloroquine in the second dimension of electrophoresis was adjusted to optimize the resolution of topoisomers over either moderate or high values of the superhelix density, $|\sigma|$. In the case of each plasmid, both two-dimensional gels show a smooth continuous pattern of topoisomer bands. We conclude from the smooth continuous behavior of bands in the two-dimensional gel pattern that no cooperative supercoiling-dependent changes in DNA twist occur over the range of superhelix densities examined.

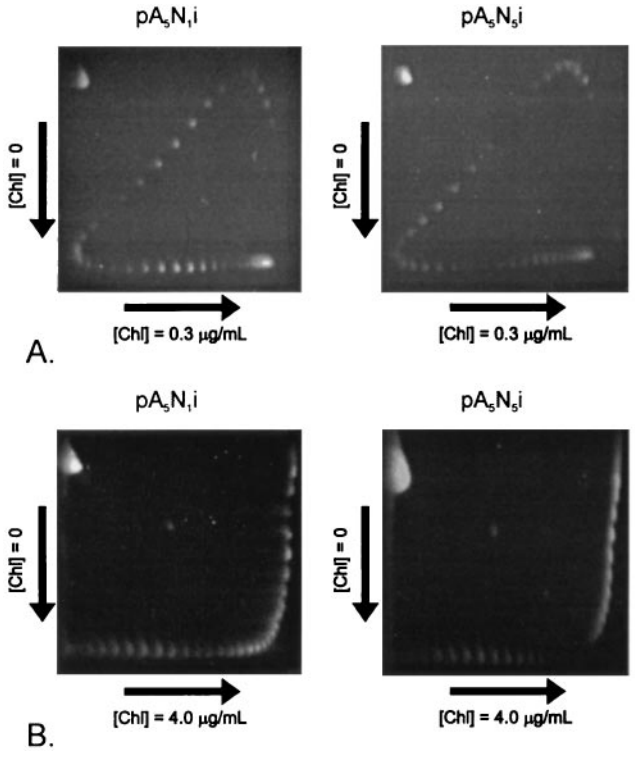

FIG. 3. Two-dimensional gel electrophoresis of pA_5N_5i and pA_5N_1i topoisomers. Mixtures of topoisomers prepared by relaxation of native supercoiled plasmids with wheat-germ topoisomerase I in the presence of ethidium bromide were subjected to agarose gel electrophoresis. First-dimension electrophoresis in all cases was carried out in TBE buffer containing 50 mM NaCl for 11 h with buffer recirculation. (*A*) Second-dimension electrophoresis carried out in TBE buffer containing chloroquine phosphate (0.3 μg/ml). (*B*) Second-dimension electrophoresis carried out in TBE buffer containing chloroquine (4 μg/ml).

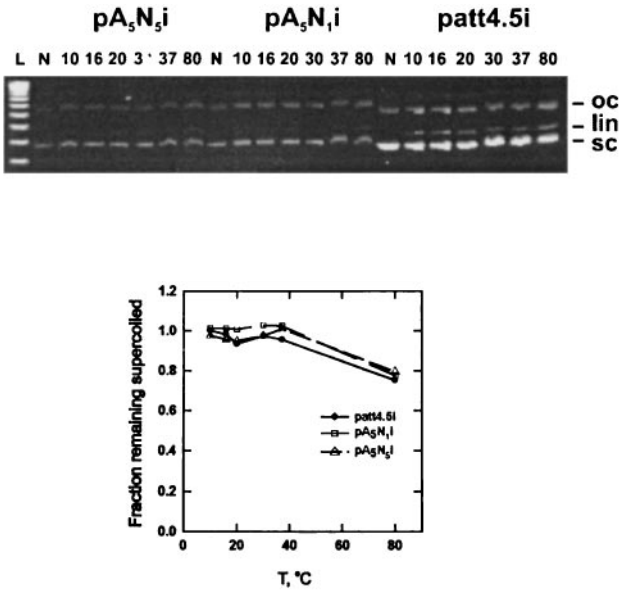

FIG. 4. Susceptibility of natively supercoiled recombination substrates to S1 nuclease digestion. L, 1-kb ladder fragments; N, native plasmid; oc, open-circular; lin, linear; sc, supercoiled plasmid. The graph shows the ratio of supercoiled plasmid remaining after 30 min of S1 digestion at the specified temperature to the amount present before the addition of S1 nuclease.

We next examined the susceptibility of the A-tract-containing plasmids to S1 nuclease digestion, which is a sensitive probe of local denaturation in supercoiled DNA. S1 digestion is a suitable technique for revealing the presence of cruciforms, B–Z junctions, and other unusual structures (37, 38). It can be seen in Fig. 4 that incubation of the two A-tract-containing plasmids and the parent plasmid p*att*4.5i at temperatures up to 37°C failed to generate any significant degree of S1 sensitivity in either of these molecules. Positive controls, in which the three plasmids were incubated at 80°C, showed significant and similar levels of S1 sensitivity. However, the S1-sensitive sites in all three plasmids were found by restriction analysis to be identical and to map to a site near the plasmid origin of replication (data not shown). We therefore conclude that S1-nuclease sensitivities in the A-tract-containing plasmids are indistinguishable from that of the parent plasmid, which lacks A-tracts.

We considered several other possible explanations for the unusual phasing-independent behavior of the A-tract-containing plasmids, such as preferential binding of IHF or Int to the A-tract inserts. These proteins cause substantial bending of DNA when bound to their specific binding sites and might, therefore, bias the knot distributions if significant binding and bending takes place at the A-tract loci. Several electrophoretic mobility shift experiments were done to measure the ability of supercoiled A-tract-containing plasmids lacking specific binding sites for IHF or Int to compete for the binding of these proteins to a linear DNA fragment containing the *attP* site, which has multiple binding sites for both Int and IHF (39). The affinity of the A-tract plasmid for the recombination proteins was extremely low and similar to that of an otherwise identical plasmid that lacked A-tracts (data not shown).

Properties of A-Tract-Containing Molecules Are Dependent on the Level of Supercoiling. Recombination-product distributions were obtained by using plasmid DNA with an average superhelix density adjusted to $\sigma = -0.03$ by relaxation with topoisomerase I in the presence of ethidium bromide. The distributions of products obtained at the same incubation temperatures as in Fig. 2 are shown in Fig. 5. At this low superhelix density, fewer knotted products are visible; how-

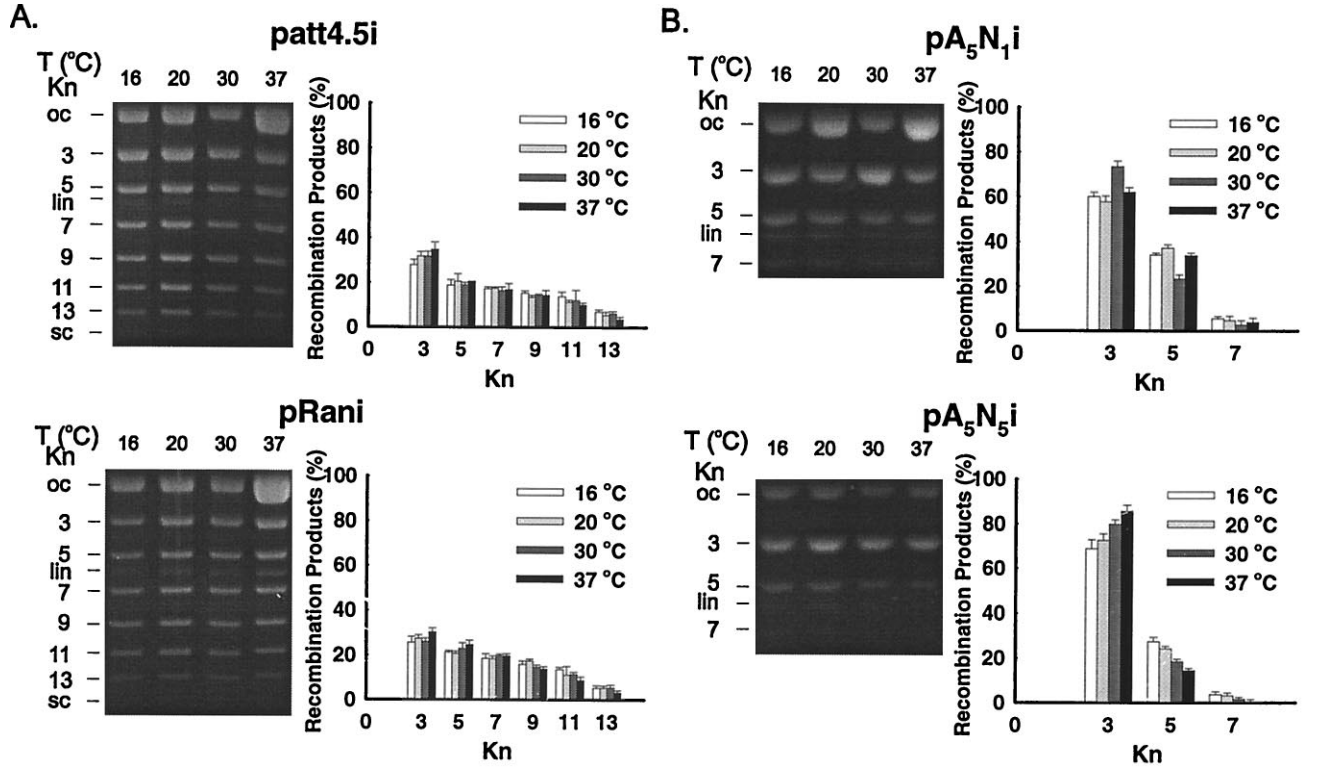

FIG. 5. Recombination-product distributions at reduced superhelix density ($\sigma_{avg} = -0.030 \pm 0.005$). (*A*) Control plasmids. (*B*) A-tract-containing plasmids. Reduced superhelix-density substrates were prepared by relaxing natively supercoiled plasmids with topoisomerase I in the presence of ethidium bromide. Superhelix densities were determined by one-dimensional agarose gel electrophoresis in the presence of chloroquine. Recombination reaction conditions and figure annotations are identical to those in Fig. 2.

ever, it can be seen that the reduction in $|\sigma|$ somewhat increases the complexity and alters the temperature dependence of the knot distribution for pA_5N_1i relative to pA_5N_5i. We interpret this differential phasing-dependent effect as an indication that pA_5N_1i returns to a structure more closely resembling "normal" DNA at higher values of $|\sigma|$ than does pA_5N_5i. However, a complete understanding of this behavior must await further characterization of the effects of superhelical stress on A-tract structure.

Analysis of Recombination-Product Distributions According to a "Biased Slithering" Model. The elastic properties of the inserted DNA sequences can be analyzed in terms of the observed knot distributions by applying a simple model for recombination-site diffusion. We assume that the slithering motion (Fig. 1) samples all possible configurations of the recombination sites in a rigid idealized superhelical structure. Our "biased slithering" model is a modified version of previous ones proposed by Benjamin and Cozzarelli (21) and Boles *et al.* (22) and incorporates preferential localization of specified sequence elements. This was done by favorably weighting those configurations in which the specified segment of the DNA contour is found in one of the end loops.

The statistical weight of end-loop-localized configurations, ξ, is equivalent to the value of an equilibrium constant for moving the specified segment into a loop from any location within the plectonemic region of the superhelix. Results of calculations using this model are shown in Fig. 6, which shows the dramatic effect of weighting localized configurations on the knot product distribution. Although the model is quite simple, the calculated distributions gave very good semiquantitative agreement with our experimental results. By using a ξ value equal to 30, we calculate an approximate 4-fold increase in the proportion of trefoil (three-noded) knots relative to the unbiased distribution at $\sigma = -0.06$ and an approximately 2.5-fold increase at $\sigma = -0.03$. Both of these estimates agree reasonably well with the experimental profiles of knot distributions shown in Figs. 2 and 5.

The value of ξ can be related to the difference in bending energy for the elastically anomalous DNA segment relative to surrounding DNA. This elastic energy, Δg_B, can be calculated from the expression $\Delta g_B = -k_B T \ln \xi$. A ξ value of 30 equates with a difference in elastic energy of about -2 kcal/mol (1 cal = 4.184 J). This elastic energy change is only a few percent of the overall difference in conformational free energy attributable to supercoiling (4, 40).

DISCUSSION

The detailed structural basis of supercoiling-dependent A-tract behavior remains unknown but may be related to a temperature-dependent structural transition in A-tract DNA observed with circular dichroism and calorimetric methods (34). In an early topological study, Diekmann and Wang (41) observed that the measured helical repeat of A-tract-containing DNA fragments isolated from *Leishmania* kinetoplast DNA was dependent on the magnitude and sign of the linking difference. They ascribed this effect to distortions of A-tract structure induced by low levels of DNA supercoiling.

The change in A-tract flexibility induced by negative supercoiling can be estimated in terms of the difference in persistence length between the superhelically distorted A-tract-containing segment and flanking DNA. The elastic energy of a weakly bending rod, Δg_B, is given by

$$\Delta g_B = \frac{\alpha}{2} \int_0^{\ell} \left(\frac{\partial \theta}{\partial s} \right)^2 ds, \qquad [1]$$

where α is the elastic force constant, θ is the local bending angle, s is an arc-length parameter, and ℓ is the contour length of the segment in question (42). The value of α is related to the

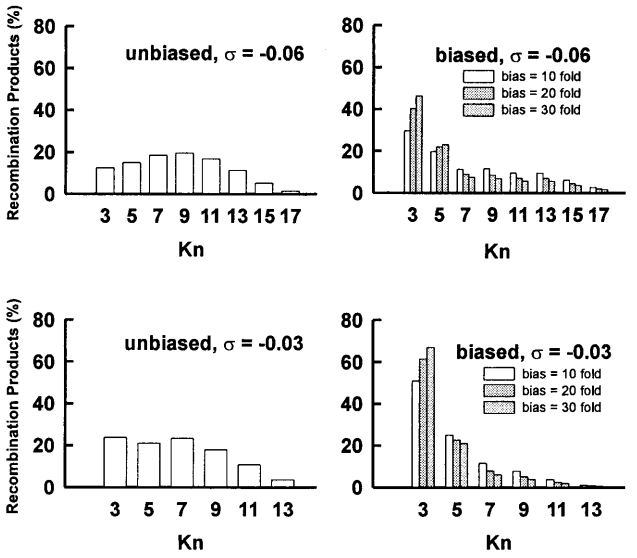

FIG. 6. Calculated knot distributions based on the biased slithering model for intramolecular site-specific recombination of a supercoiled Int substrate. Histograms on the left show the distribution of knots obtained for cases in which there are no sequence-dependent preferences for looped regions; profiles on the right correspond to different end-loop biases, ξ, equal to 10, 20, or 30. Model parameters were based on a 4.60-kb DNA substrate divided into 950-bp and 3.65-kb domains. Recombination substrates were considered to be a heterogeneous population of superhelical molecules with mean values of the linking difference corresponding to high ($\sigma = -0.06$) or low ($\sigma = -0.03$) superhelix density; this heterogeneity was assumed to obey a Gaussian distribution with variances equal to the experimentally measured values obtained from topoisomer distributions of plasmid substrates. Conformations in which a superhelix end loop was partially occupied by the biased DNA segment were weighted according to their elastic energy, as given in Eq. **1**.

chain persistence length, P, through the relationship $\alpha = k_B TP$, where k_B is Boltzmann's constant and T is the absolute temperature. After integrating the above expression, the apparent difference in persistence length of the supercoiled A-tract-containing segment relative to flanking DNA, ΔP, is then given in terms of the difference in bending energy, $\Delta\Delta g_B$ by

$$\frac{\Delta\Delta g_B}{k_B T} = \frac{\Delta P \theta^2}{2\ell}. \qquad [2]$$

An estimate of ΔP was found by assuming that the 105-bp insert was bent into a regular semicircle at the end of the superhelix. If there is no residual contribution from intrinsic bending, then the effective persistence length of the A-tract region decreases from an assumed value of 50 nm in the relaxed state to about 25 nm at $\sigma = -0.06$.

To our knowledge, the topological experiments described herein provide the first direct evidence for supercoiling-dependent changes in the bending and flexibility of particular DNA sequences and may provide a basis for understanding the role of A-tract structure in transcriptional activation.

We thank N. R. Cozzarelli, H. A. Nash, and C. Robertson for gifts of recombination proteins and for plasmid-bearing strains; J. Gardner for providing the Int expression system EM424/pSX-1; C. Ross for assistance with protein purification; and N. R. Cozzarelli, W. K. Olson, and P. H. von Hippel for their comments on the manuscript. This work was supported by a grant from the National Institutes of Health (GM47898) to S.D.L.

1. Vologodskii, A. V. & Cozzarelli, N. R. (1994) *Annu. Rev. Biophys. Biomol. Struct.* **23,** 609–643.
2. Levene, S. D. (1994) in *Nucleic Acids and Molecular Biology,* eds. Eckstein, F. & Lilley, D. M. J. (Springer, Heidelberg), Vol. 8, pp. 119–132.
3. Schlick, T. (1995) *Curr. Opin. Struct. Biol.* **5,** 245–262.
4. Vologodskii, A. V., Levene, S. D., Klenin, K. V., Frank-Kamenetskii, M. D. & Cozzarelli, N. R. (1992) *J. Mol. Biol.* **227,** 1224–1243.
5. Pérez-Martín, J., Rojo, F. & de Lorenzo, V. (1994) *Microbiol. Rev.* **58,** 268–290.
6. McAllister, C. F. & Achberger, E. C. (1988) *J. Biol. Chem.* **263,** 11743–11749.
7. McAllister, C. F. & Achberger, E. C. (1989) *J. Biol. Chem.* **264,** 10451–10456.
8. Bracco, L., Kotlarz, D., Kolb, A., Diekmann, S. & Buc, H. (1989) *EMBO J.* **8,** 4289–4296.
9. Kim, J., Klooster, S. & Shapiro, D. J. (1995) *J. Biol. Chem.* **270,** 1282–1288.
10. Gartenberg, M. R. & Crothers, D. M. (1991) *J. Mol. Biol.* **219,** 217–230.
11. Ellinger, T., Behnke, D., Knaus, R., Bujard, H. & Gralla, J. D. (1994) *J. Mol. Biol.* **239,** 466–475.
12. Brahms, G., Brahms, S. & Magasanik, B. (1995) *J. Mol. Biol.* **246,** 35–42.
13. Laundon, C. H. & Griffith, J. (1988) *Cell* **52,** 545–549.
14. Langowski, J., Olson, W. K., Pedersen, S. C., Tobias, I., Westcott, T. P. & Yang, Y. (1996) *Trends Biochem. Sci.* **21**, 50.
15. Yang, Y., Tobias, I. & Olson, W. K. (1993) *J. Chem. Phys.* **98,** 1673–1686.
16. Bauer, W. R., Lund, R. A. & White, J. H. (1993) *Proc. Natl. Acad. Sci. USA* **90,** 833–837.
17. Tobias, I. & Olson, W. K. (1993) *Biopolymers* **33,** 639–646.
18. Zhang, P., Tobias, I. & Olson, W. K. (1994) *J. Mol. Biol.* **242,** 271–290.
19. Klenin, K. V., Frank-Kamenetskii, M. D. & Langowski, J. (1995) *Biophys. J.* **68,** 81–88.
20. Rippe, K., von Hippel, P. H. & Langowski, J. (1995) *Trends Biochem. Sci.* **20,** 500–506.
21. Benjamin, H. W. & Cozzarelli, N. R. (1986) *Proc. Robert A. Welch Found. Conf. Chem. Res.* **29,** 107–126.
22. Boles, T. C., White, J. H. & Cozzarelli, N. R. (1990) *J. Mol. Biol.* **213,** 931–951.
23. Bliska, J. B. & Cozzarelli, N. R. (1987) *J. Mol. Biol.* **194,** 205–218.
24. Sambrook, J, Fritsch, E. F. & Maniatis, T. (1989) *Molecular Cloning: A Laboratory Manual* (Cold Spring Harbor Lab. Press, Plainview, NY), 2nd Ed.
25. Nash, H. A. (1983) *Methods Enzymol.* **100,** 210–216.
26. Nash, H. A., Robertson, C. A., Flamm, E., Weisberg, R. A. & Miller, H. I. (1987) *J. Bacteriol.* **169,** 4124–4127.
27. Levene, S. D. & Tsen, H. (1996) in *Protocols in DNA Topology and Topoisomerases,* eds. Bjornsti, M. & Osheroff, N. (Humana, Totowa, NJ), Vol. 1, in press.
28. Barzilai, R. (1973) *J. Mol. Biol.* **74,** 739–742.
29. Dynan, W. S., Jendrisak, J. J., Hager, D. A. & Burgess, R. R. (1981) *J. Biol. Chem.* **256,** 5860–5865.
30. Bowater, R., Aboul-ela, F. & Lilley, D. M. J. (1992) *Methods Enzymol.* **212,** 105–120.
31. Bowater, R. P., Aboul-ela, F. & Lilley, D. M. J. (1994) *Nucleic Acids Res.* **22,** 2042–2050.
32. Crothers, D. M., Haran, T. E. & Nadeau, J. G. (1990) *J. Biol. Chem.* **265,** 7093–7096.
33. Marini, J. C., Effron, P. N., Goodman, T. C., Singleton, C. K., Wells, R. D., Wartell, R. M. & Englund, P. T. (1984) *J. Biol. Chem.* **259,** 8974–8979.
34. Levene, S. D., Wu, H.-M. & Crothers, D. M. (1986) *Biochemistry* **25,** 3988–3995.
35. Chan, S. S., Breslauer, K. J., Austin, R. H. & Hogan, M. E. (1993) *Biochemistry* **32,** 11776–11784.
36. Wang, J. C., Peck, L. J. & Becherer, K. (1983) *Cold Spring Harbor Symp. Quant. Biol.* **47,** 85–92.
37. Sullivan, K. & Lilley, D. M. J. (1986) *Cell* **47,** 817–827.
38. Wohlrab, F. (1992) *Methods Enzymol.* **212,** 294–301.
39. Landy, A. (1989) *Annu. Rev. Biochem.* **58,** 913–949.
40. Horowitz, D. S. & Wang, J. C. (1984) *J. Mol. Biol.* **173,** 75–91.
41. Diekmann, S. & Wang, J. C. (1985) *J. Mol. Biol.* **186,** 1–11.
42. Landau, L. D. & Lifshitz, E. M. (1986) *Theory of Elasticity,* (Butterworth–Heinemann, Boston), 3rd Ed., pp. 67–70.